



Original Research Article

Isotherms, Kinetics, Equilibrium, and Thermodynamic Studies on the Uptake of Hexavalent Chromium Ions from Aqueous Solution Using Synthetic Hydroxyapatite

Aborode Abdullahi Tunde¹, Benedicta Donkor^{2,3}, Abigail Owusuwaa Gyamfi^{2,4} and Ernest Opoku^{*2,3}

¹Department of Chemistry, University of Ilorin, Ilorin, Nigeria

²Department of Basic and Computational Sciences, Koachie Health Systems, Accra, Ghana

³Department of Chemistry and Biochemistry, Auburn University, Auburn, Alabama 36849-5312, USA

⁴Department of Occupational and Environmental Health and Safety, School of Public Health, Kwame Nkrumah University of Science and Technology, Kumasi, Ghana

ARTICLE INFO

Article history

Submitted: 2020-06-24

Revised: 2020-07-24

Accepted: 2020-08-14

Available online: 2020-09-13

Manuscript ID: [AJCB-2006-1050](#)

DOI: [10.22034/ajcb.2020.113974](https://doi.org/10.22034/ajcb.2020.113974)

KEYWORDS

Chromium

Hydroxylapatite

Adsorption

Isotherms

ABSTRACT

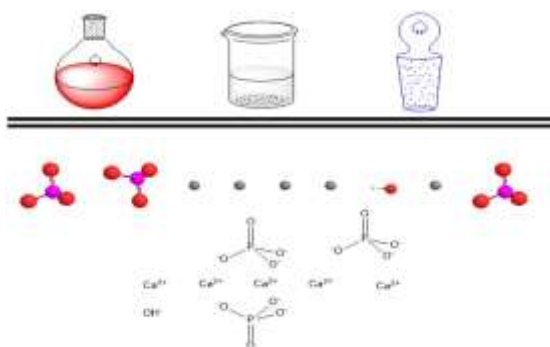
The effective and economic removal of heavy metals from industrial effluents is one of the important issues globally. In this study, hydroxyapatite (HAP) was synthesized using the wet chemical precipitation method and was characterized using Fourier transform infrared (FTIR) spectroscopy, UV-Visible spectrometry, scanning electron microscopy (SEM) and X-ray diffraction (XRD) methods. Different physico-chemical parameters of the HAP such as color, bulk density, and pH were determined. Removal efficiency of Cr(VI) was investigated by different parameters such as initial concentration, contact time, pH, adsorbent dosage and temperature. Results showed that the adsorption of Cr(VI) was favorable in acidic medium. Adsorption kinetics using pseudo-first order and pseudo-second order kinetic models were tested on the experimental data. The Kinetics of the adsorption followed a pseudo-second order kinetics model as we obtained a higher correlation coefficient value of $R^2 = 0.978$. The equilibrium data were evaluated using two adsorption isotherms: Langmuir and Freundlich adsorption isotherms. The equilibrium data fitted well with Langmuir adsorption isotherm model, showing monolayer coverage of Cr(VI) ions over the surface of HAP and this fact is supported by the Langmuir isotherm plot and the correlation coefficient value of $R^2 = 0.9639$.

* Corresponding author: Opoku, Ernest

✉ E-mail: ernopoku@gmail.com

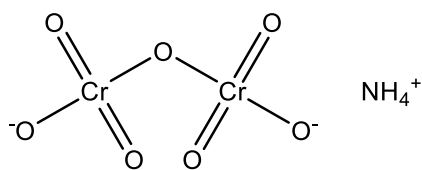
© 2020 by SPC (Sami Publishing Company)



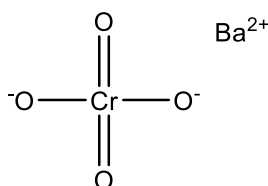
GRAPHICAL ABSTRACT

1 Introduction

Heavy metals are metals and/or metallic compounds that may harm human health when absorbed or inhaled [1]. In very small amounts, some heavy metals support life. However, when heavy metals are taken in large amounts, they can become toxic. Heavy metal contamination is an environmental threat as serious as global warming. Examples of heavy metals include arsenic, cadmium, chromium, copper, lead, mercury and zinc. Generally, heavy metals have densities above 5 g/cm³ [2,3]. Hydroxyapatite (HAP) is a naturally occurring mineral from calcium apatite with the formula Ca₅(PO₄)₃OH but can also be written as Ca₁₀(PO₄)₆(OH)₂ to denote that the crystal unit cell has two entities. HAP can be synthesized by different methods [4–6] such as the wet chemical precipitation method, or from biomaterials such as eggshells [7]. HAP is present in bone and teeth [4], it has medical application in bone grafting materials, hips replacement, dental implants among others. HAP from human and animal remains are used in archaeology to reconstruct ancient diets, migrations and paleoclimate. The mineral fractions of bones and teeth acts as a reservoir of trace elements like carbon, oxygen and strontium [8–11]. HAP also have applications in adsorption process with specificity in wastewater purification and remediation [12,13]. The term adsorption refers to the accumulation of a substance at the interface between two phases

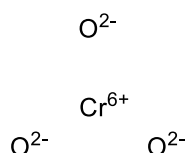
(liquid-solid interface or gas-solid interface) [14]. The substance that accumulates at the interface is called adsorbate and the solid on which adsorption occurs is adsorbent [15]. Adsorption is a surface-based process while absorption involved the assimilation of molecular species throughout the bulk of the solid or liquid. An adsorbent is a liquid or solid on which the adsorbate accumulates during the adsorption process, and adsorbate is a substance which is adsorbed on the surface of an adsorbent. Adsorption are classified into two types; chemical sorption and physical sorption [15]. Adsorption has been employed as a chemical technique for mitigating against environmental and chemical contaminants. Several studies exist in the literature where adsorption process have been employed to remove various materials as a means of purification and separation. It has been well established that all hexavalent chromium compounds are toxic (due to their oxidizing power) as well as carcinogenic [16]. Hexavalent chromium compounds are among the leading causes of lung cancer, especially when they are airborne [17]. In addition, positive associations have been found between human exposure to chromium (VI) compounds and cancer of the nose and nasal sinuses [18]. Scheme 1 below illustrates examples of chromium (VI) complexes.

NH₄⁺

Ammonium dichromate



Barium chromate



Chromium trioxide

Scheme 1: examples of chromium (VI) complexes

Therefore, there is the need to search for an eco-friendly and low-cost means of getting rid of hexavalent chromium compounds from the environment. A search of the literature revealed that a few studies have been done on means of removing chromium (VI) compounds from the environment, particularly from wastewater [19,20]. Some studies also made use of zeolites and chitosan to address this challenge [21]. While these reports are robust, there is still the need for cheaper and more ecofriendly alternatives to complement the gains made so far [22]. Therefore, we report herein a simple, user- and ecofriendly method for the removal of hexavalent compounds in aqueous solutions. Specifically, we investigate the adsorption of chromium (VI) from aqueous solution using

hydroxyapatite. Hydroxyapatite has been found to be a reliable and cheaper adsorbent for removal of cesium and strontium ions from aqueous solutions [23,24]. Zamani and co-workers have also reported the use of hydroxyapatite to effectively remove nickel ions from aqueous solutions [25]. Our study is extrapolated by exploring the kinetics, thermodynamics and equilibrium of the adsorption process. Furthermore, we also investigate the appropriate isotherm that governs this adsorption process. The advances obtained from the kinetics, thermodynamics, equilibrium and isotherm studies are crucial towards providing a sound theoretical insight into the adsorption capability of the hydroxyapatite. The theoretical insights [26] gained are necessary to consolidate with the present literature whiles providing guidance for correlative applications, experiments and future extensions.

2 Materials and Methods

2.1 Materials

The main reagents used in this study are Calcium hydroxide $\text{Ca}(\text{OH})_2$, orthophosphoric acid (H_3PO_4), deionized water, ammonium hydroxide (NH_4OH), potassium dichromate salt ($\text{K}_2\text{Cr}_2\text{O}_7$), and Hydrochloric acid (HCl). All the chemicals used were of analytical grade and required no further purification and treatment. All chemicals were obtained from Sigma Aldrich, Germany.

2.2 Methods

2.2.1 Preparation of Adsorbent (HAP)

Hydroxyapatite was synthesized using the wet chemical precipitation method [27], Calcium hydroxide ($\text{Ca}(\text{OH})_2$), Orthophosphoric acid (H_3PO_4) were used as Ca and P precursors with mole ratio of 10:6. Initially, 0.6 mol of H_3PO_4 400ml was added dropwise into 1.0 mol ($\text{Ca}(\text{OH})_2$ 750ml with vigorous stirring. During titration,

the pH of the mixture was monitored and maintained above 10.5 by adding ammonium hydroxide (NH₄OH). After titration, the solution was continuously stirred for 5 hours at room temperature before being filtered and washed using deionized water. The residue was oven dried at 60°C for 24hr. The dried cake was then crushed using mortar and pestle to obtain well-defined HAP powder.

2.2.2 Preparation of adsorbate

The stock solution of Cr(VI) was prepared by dissolving 0.283g potassium dichromate salt (K₂Cr₂O₇) in 100ml of deionized water. Various standards (0 - 500ppm) were prepared from the stock solution by dilution. The Shimadzu (UVmini-1240) UV/Visible spectrophotometer was used to first determine the maximum wavelength of the solution and the absorption maxima λ_{\max} was at 350 nm. The UV/Visible spectrophotometer was set to this wavelength which was then used for subsequent experiments.

2.2.3 Adsorption Experiments

Adsorption of Cr(VI) ions were carried out in batch process with initial concentration ranged from 0 ppm to 500 ppm. Batch adsorption experiments were carried out with 20 ml of solution of the adsorbate. Adsorbent (HAP) of 0.02g was weighed and carefully transferred into conical flasks and 20ml of each concentration of the adsorbate Cr(VI) was measured into the flask and correctly labelled. The labelled flasks were covered with aluminum foil and placed in the water bath shaker and the time was set to 240 minutes at room temperature (39°C) at 200 rpm (revolution per minutes). After shaking, the samples were brought out and filtered into labelled bottles.

Then the filtrate after various adsorption processes were analyzed by UV-Vis

Spectrophotometer under visible lamp range with a wavelength of 350 nm.

2.2.4 Equilibrium adsorption capacity and uptake efficiency

The amount of Cr(VI) adsorbed at equilibrium was calculated using the equation $Q_e = \left(\frac{C_i - C_e}{M}\right)V$, where, C_i and C_e are the initial and final Cr(VI) concentrations (mg/L) of the solution in each adsorption experiment. V is the volume of the chromium solution in liters, and Q_e is in mg/g. The exact dosage of the adsorbent needed to sufficiently remove the Cr(VI) was determined.

3 Results and Discussion

3.1 Characterization of HAP

3.1.1 FTIR results

Functional groups associated with the synthesized hydroxyapatite were identified by FTIR spectroscopy. The FTIR spectrum of the prepared sample is given in Fig.1. The vibrational stretch of frequency 3568 cm⁻¹ confirms the presence of a hydroxyl fragment. Likewise, the other stretching vibrations for carbonyl and phosphate groups were also observed as clearly shown in Fig.1. The FTIR results of the synthesized hydroxyapatite in this work compares favorably with those in literature [28].

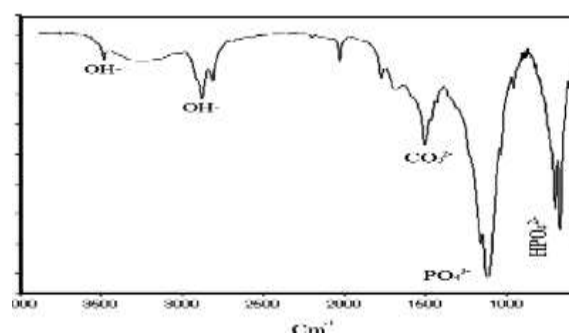


Fig. 1: FTIR results of synthesized hydroxyapatite.

3.1.2 SEM analysis

The scanning electron microscope (SEM) was used for the morphological study of the hydroxyapatite. Fig. 2 shows the SEM images of the synthesized hydroxyapatite. It is observed that the hydroxyapatite nanoparticles formed are highly agglomerated in good agreement with other reports [27,29]. The spherical shaped particles with clumped distributions are visible from the analysis.

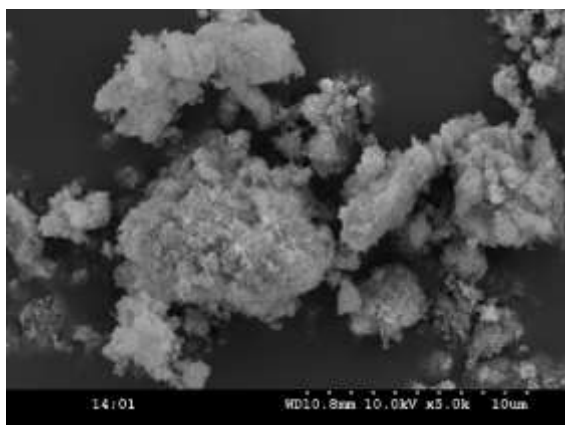


Fig. 2: SEM analysis results of synthesized hydroxyapatite

3.1.3 X-ray Diffraction (XRD) results

The diffraction patterns were collected over a 2θ range from 2.000° to 79.9850° with an incremental step size of 0.0450° using flat plane geometry. The acquisition time was set at 0.7 seconds for each scan. The main (h k l) indices for nano HAP: (3.02731), (2.78986), (1.92143) being indicated. Comparing the results with Shahabi *et al* [30], high intensity occurs at $2\theta = 30$ and 35 and high h k l values at $2\theta = 45$ to 50 . This shows that the spectrum obtained from the XRD (Fig. 3) gives the structural parameters and the structural identification for standard HAP.

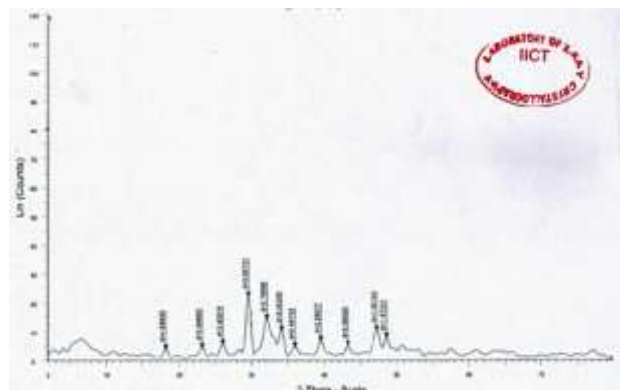


Fig. 3: XRD analysis results of synthesized hydroxyapatite.

3.2 Results on Adsorption Experiment

3.2.1 Effect of initial adsorption concentration

Fig. 4 below indicates that as the % absorbance of the sample analyzed increases the concentration of the sample analyzed increases which result in the discussion that increase in the % absorbance of the sample lead to increase in the concentration and vice versa.

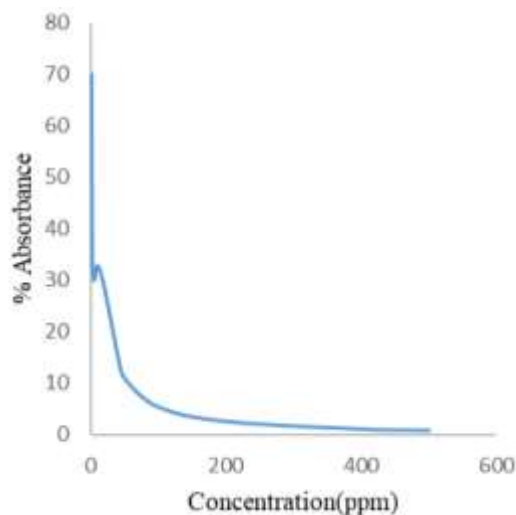


Fig. 4: Absorbed and concentration

3.2.2 Effect of adsorbent dosage

Fig. 5 below explain the results obtained on the sample analyzed when the adsorbent dosage had strongly affected the sorption capacity. With the fixed metal ions concentration, the percentage removal of metal ions in the sample analyzed increased with increasing weight of the adsorbents. This was due to more availability of active sites or surface area at higher concentration of adsorbent. Different weight of the adsorbent was weighed (0.02g, 0.004g, 0.05g, 0.06g, 0.08g, 0.1g, 0.2g, 0.4g, 0.5g, 0.8g) and 20 ml of [Cr(VI) solution] optima concentration (40 ppm) which gave the highest absorbance was added to it in a conical flask and placed in the bath shaker for 2hrs.

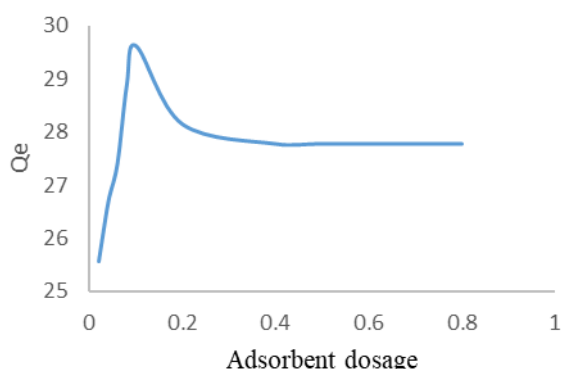


Fig. 5: Effect of adsorbent dosage

3.2.3 Effect of pH

Fig. 6 shows the effect of initial Cr(VI) concentration on equilibrium pH. The exact dosage of adsorbent obtained from the study of effect of adsorbent dosage was weighed and 20 ml of the optimum concentration of the [Cr(VI) solution] at different pH ranging from 2-3 for Cr(VI), was added into the conical flask. The pH of the [Cr (VI) solution] was adjusted by adding HCl or NaOH and the pH values were checked by the pH meter whiles the solutions was shaken for 2 hours and filtered. It was observed that, the equilibrium adsorption concentration increased sharply at pH 2.0 and begin to decline at a near 3.0 pH. This observation suggests that, the

optimum pH for adsorption of the Cr(VI) ions by HAP in aqueous solutions lies in the range of 2.0 and 3.0.

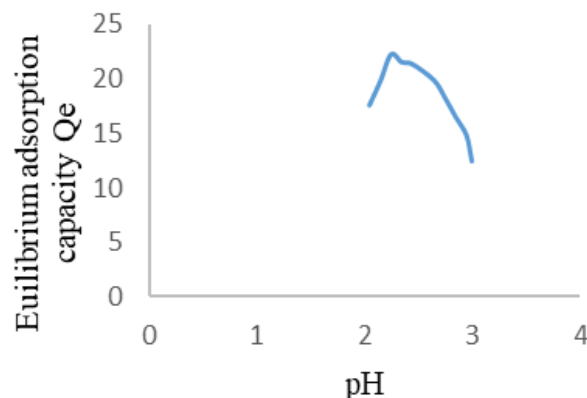


Fig. 6: Effect of pH

3.2.4 Effect of contact time

Fig. 7 below indicates the result obtained when concentration of the adsorbate with the highest absorbance (600 ppm) was used when 0.02 g of the adsorbent (HAP) is measured and are added in a conical flask and placed in a bath shaker. It is made to rotate at different time.

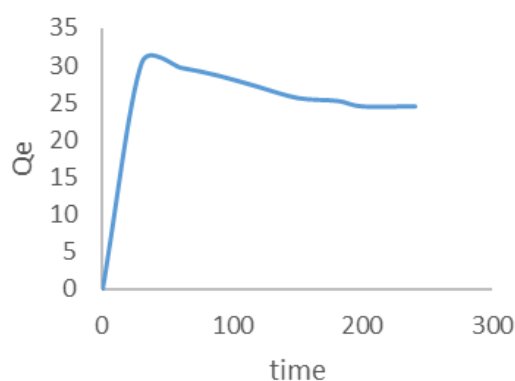


Fig. 7: Effect of time (min)

3.2.5 Effect of temperature

Fig. 8 indicate the result obtained when the concentration of the Cr (VI) solution was used. As the adsorption capacity concentration of the sample analyzed increases, the temperature

increases, this explained that increase in the concentration of the adsorption capacity of the sample result to increases in the temperature.

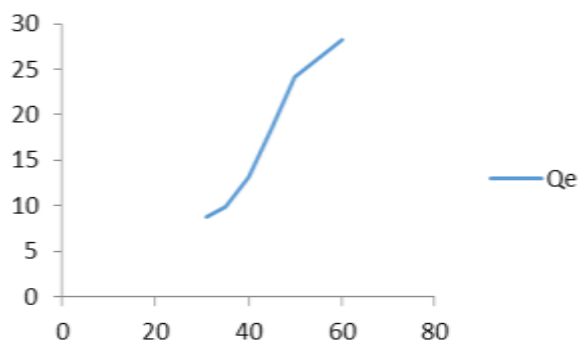


Fig. 8: Graph of temperature against equilibrium adsorption capacity

3.3 Adsorption Isotherms

3.3.1 Langmuir Isotherm

The Langmuir adsorption model is based on the assumption that maximum adsorption corresponds to a saturated monolayer of solute molecules on the adsorbent surface, with no lateral interaction between the adsorbed molecules [31]. The Langmuir adsorption isotherm has been successfully used in many monolayer adsorption processes. Adsorption isotherms describe the interaction of adsorbates with adsorbents. The linear form of Langmuir equation [32] and separation factor are given as follow

$$\frac{c_e}{q_e} = \frac{1}{k_L q_{max}} + \frac{1}{q_{max}} c_e$$

$$R_L = \frac{1}{1 + k_L c_0}$$

Where q_e is the amount adsorbed per adsorbent mass (mg/g), C_e is the equilibrium concentration of the adsorbate (mg/L), K_L is the Langmuir's constant and q_{max} is the maximal adsorption efficiency (mg/g). The adsorption is feasible when R_L value falls between the range, $0 < R_L < 1$. The Langmuir plot in **Fig.9** shows that the adsorption process conforms to the model with

R^2 value of 0.9639. This implies that the adsorption process is well described through the Langmuir mechanism.

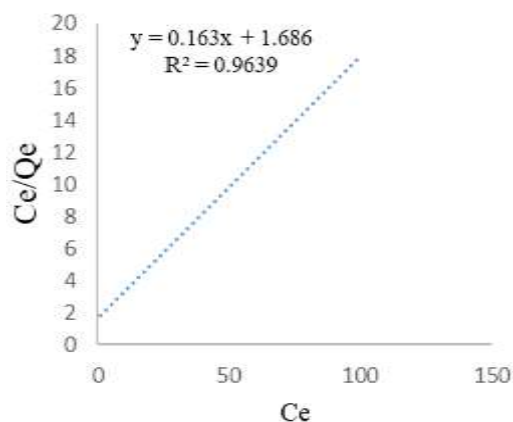


Fig. 9: Langmuir adsorption isotherm for Cr (VI) removal

3.3.2 Freundlich Isotherm

We now proceed to test our adsorption process on the Freundlich isotherm. The Freundlich model can be applied to multilayer adsorption with non-uniform distribution of adsorption heat and affinities over a given heterogeneous surface [33]. In this case, the experimental data were analyzed by Freundlich isotherm model [34] in the linearized form using equation 4:

$$\log q_e = \frac{1}{n} \log C_e + \log KF \tag{4}$$

Where KF is the Freundlich adsorption constant and it is the maximum adsorption capacity of metal ions (mg/g) and n is the constant which illustrates the adsorption intensity. **Fig.10** indicate the Freundlich adsorption isotherm for Cr(VI) removal as the adsorption heat of the concentration increases the concentration also increases, this help to calculate the Langmuir and Freundlich adsorption isotherms.

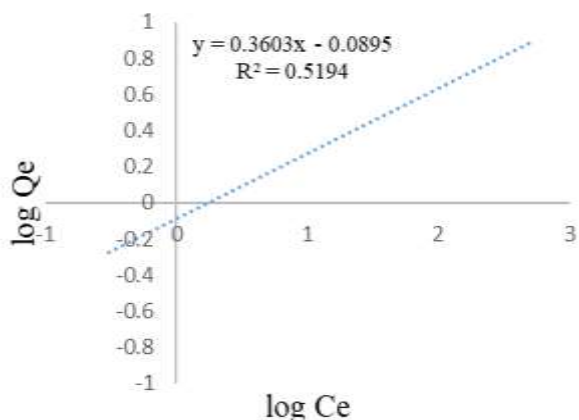


Fig. 10: Freundlich adsorption isotherm for Cr(VI) removal

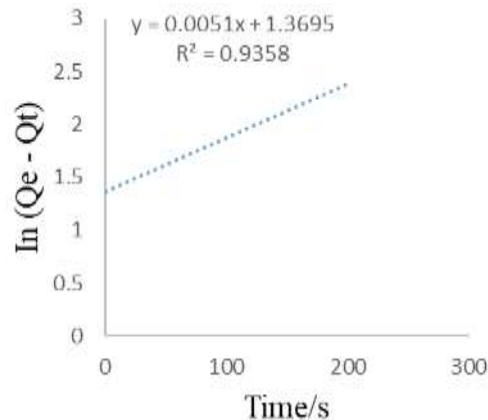


Fig. 11: Pseudo-first order kinetics of Cr(VI) on HAP

The equilibrium data fitted well with Langmuir Adsorption Isotherm Model, showing monolayer coverage of Cr(VI) ions over the surface of HAP and this fact is supported by the Langmuir Isotherm plot and the Correlation Co-efficient value of $R^2 = 0.9639$ was obtained.

3.4 Adsorption Kinetics

Pseudo-first order and pseudo-second order were used to analyze the kinetics of Cr(VI) adsorption onto HAP. The kinetics of adsorption data were processed to understand the dynamics of adsorption process in terms of rate constant order.

3.4.1 Pseudo-First Order Kinetics

The pseudo-first order kinetics plot for adsorption of Cr(VI) onto HAP is shown in Fig. 11. It is observed from Fig. 11 that the relationship between the Cr(VI) solution diffusivity, $\ln(q_e - q_t)$ against t is linear. In addition, highly linear plots with high values of correlation coefficient ($R^2 = 0.9358$) were also observed for the adsorption of Cr(VI). These results indicate that the adsorption of Cr(VI) fitted well with the pseudo-first order model and it is sufficient enough in reporting and representing the kinetics of the adsorptions.

3.4.2 Pseudo-Second Order Kinetics

The pseudo-second-order kinetics for the adsorption of Cr(VI) onto HAP. The pseudo-second-order rate constant K_2 , and Q_e determined from the model are presented. It can be observed that highly linear plots with high values of correlation coefficient ($R^2 = 0.978$) were also observed from Fig. 12 for the adsorption of Cr(VI). These results indicate that the adsorption of Cr(VI) fitted well with the pseudo-second order model and it is best sufficient enough in reporting and representing the kinetics of the adsorptions.

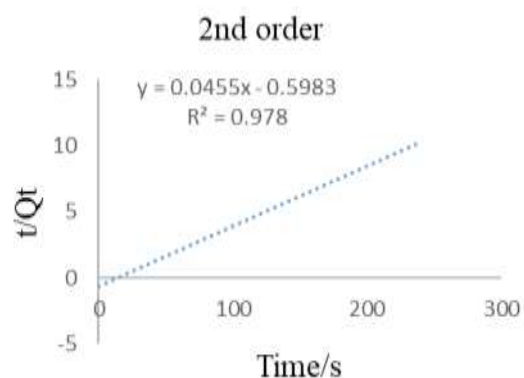


Fig. 12: Pseudo-second order kinetics of Cr(VI) on HAP

3.5 Adsorption Thermodynamics

The thermodynamic parameters for the adsorption of Cr(VI) ions by HAP were determined using the following equations:

$$Kd = \frac{qe}{Ce} \Delta G = -RT \ln Kd$$

$$\ln Kd = \frac{\Delta S}{R} - \frac{\Delta H}{RT}$$

where K_d is the distribution coefficient for the adsorption in g/L, ΔG is the Gibbs free energy in J/mol, R is the universal gas constant in J/mol K, T is the absolute temperature in K, ΔS is the entropy change in J/mol K and ΔH is the enthalpy change in kJ/mol. **Fig. 13** indicate the adsorption thermodynamics of the sample analyzed which indicate the spontaneous nature of the sample.

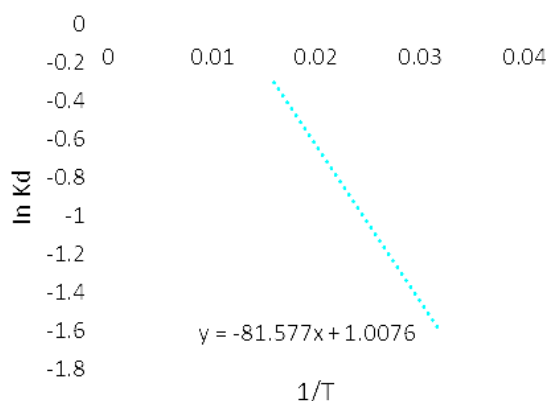


Fig. 13: Adsorption Thermodynamics

Fig. 13 explained more about the positive values of Gibbs free energy change (ΔG) obtained for the adsorption of Cr (VI) ions by HAP at various temperatures had shown the non-spontaneous nature of the adsorption process. The negative values of enthalpy change (ΔH°) obtained for the adsorption of Cr (VI) ions by HAP at various temperatures indicated that the adsorption reactions were exothermic. The positive values of entropy change (ΔS°) for the adsorption of Cr (VI) ions by HAP at various temperatures showed the increased randomness at solid-liquid

interphase during the sorption processes of Cr(VI) ions on the adsorbent.

4 Conclusion

The present study concludes that the HAP is a cheaper, ecofriendly and effective adsorbent for the removal of Cr(VI) ions from aqueous solution. The adsorption process was influenced by the pH medium and the optimum pH was 2.5 and the concentration with the highest absorbance is 40 ppm. The equilibrium data fitted well with Langmuir adsorption isotherm model, showing monolayer coverage of Cr(VI) ions over the surface of HAP and this fact is supported by the Langmuir Isotherm plot and the correlation coefficient value of $R^2 = 0.9639$ was obtained. The Langmuir maximum adsorption capacity was found to be 6.134 (mg/g). The Kinetics of the adsorption followed a pseudo-second order kinetics model as we obtained a higher correlation coefficient value of $R^2 = 0.978$.

Acknowledgements

This work received no financial assistance.

Competing Interest

The authors declare that there is no conflict of interests whatsoever regarding this manuscript.

References

- [1] B. Volesky, Z.R. Holan, Biosorption of Heavy Metals, *Biotechnol. Prog.* 11 (1995) 235–250. <https://doi.org/10.1021/bp00033a001>.
- [2] A. Mohammed Alkheraz, A.K. Ali, K. Muftah Elsherif, Equilibrium and thermodynamic studies of Pb(II), Zn(II), Cu(II) and Cd(II) adsorption onto mesembryanthemum activated carbon, *J. Med. Chem. Sci. J. Homepage.* 3 (2020) 1–10. <https://doi.org/10.26655/JMCSMCI.2020.1.1>.
- [3] A.B. J., *Heavy Metals in Soils*, 2013.

- https://doi.org/10.1007/978-94-007-4470-7_10.
- [4] X. Zhang, K.S. Vecchio, Hydrothermal synthesis of hydroxyapatite rods, *J. Cryst. Growth.* 308 (2007) 133–140. <https://doi.org/10.1016/j.jcrysgro.2007.07.059>.
- [5] M. Sadat-Shojai, M.T. Khorasani, E. Dinpanah-Khoshdargi, A. Jamshidi, Synthesis methods for nanosized hydroxyapatite with diverse structures, *Acta Biomater.* 9 (2013) 7591–7621. <https://doi.org/10.1016/j.actbio.2013.04.012>.
- [6] R.R. Rao, H.N. Roopa, T.S. Kannan, Solid state synthesis and thermal stability of HAP and HAP - β -TCP composite ceramic powders, *J. Mater. Sci. Mater. Med.* 8 (1997) 511–518. <https://doi.org/10.1023/A:1018586412270>.
- [7] E.M. Rivera, M. Araiza, W. Brostow, V.M. Castaño, J.R. Díaz-Estrada, R. Hernández, J.R. Rodríguez, Synthesis of hydroxyapatite from eggshells, *Mater. Lett.* 41 (1999) 128–134. [https://doi.org/10.1016/S0167-577X\(99\)00118-4](https://doi.org/10.1016/S0167-577X(99)00118-4).
- [8] M. Descamps, J.C. Hornez, A. Leriche, Manufacture of hydroxyapatite beads for medical applications, *J. Eur. Ceram. Soc.* 29 (2009) 369–375. <https://doi.org/10.1016/j.jeurceramsoc.2008.06.008>.
- [9] B. Locardi, U.E. Pazzaglia, C. Gabbi, B. Profilo, Thermal behaviour of hydroxyapatite intended for medical applications, *Biomaterials.* 14 (1993) 437–441. [https://doi.org/10.1016/0142-9612\(93\)90146-S](https://doi.org/10.1016/0142-9612(93)90146-S).
- [10] N.A. Zakharov, I.A. Polunina, K.E. Polunin, N.M. Rakitina, E.I. Kochetkova, N.P. Sokolova, V.T. Kalinnikov, Calcium hydroxyapatite for medical applications, *Inorg. Mater.* 40 (2004) 641–648. <https://doi.org/10.1023/B:INMA.0000032000.83171.9f>.
- [11] J. Huang, S.M. Best, W. Bonfield, T. Buckland, Development and characterization of titanium-containing hydroxyapatite for medical applications, *Acta Biomater.* 6 (2010) 241–249. <https://doi.org/10.1016/j.actbio.2009.06.032>.
- [12] N.A. Medellin-Castillo, R. Leyva-Ramos, E. Padilla-Ortega, R.O. Perez, J. V. Flores-Cano, M.S. Berber-Mendoza, Adsorption capacity of bone char for removing fluoride from water solution. Role of hydroxyapatite content, adsorption mechanism and competing anions, *J. Ind. Eng. Chem.* 20 (2014) 4014–4021. <https://doi.org/10.1016/j.jiec.2013.12.105>.
- [13] J.W. Shen, T. Wu, Q. Wang, H.H. Pan, Molecular simulation of protein adsorption and desorption on hydroxyapatite surfaces, *Biomaterials.* 29 (2008) 513–532. <https://doi.org/10.1016/j.biomaterials.2007.10.016>.
- [14] T. Selmi, M. Seffen, H. Sammouda, S. Mathieu, J. Jagiello, A. Celzard, V. Fierro, Physical meaning of the parameters used in fractal kinetic and generalised adsorption models of Brouers–Sotolongo, *Adsorption.* 24 (2018) 11–27. <https://doi.org/10.1007/s10450-017-9927-9>.
- [15] A. Dąbrowski, Adsorption - From theory to practice, *Adv. Colloid Interface Sci.* 93 (2001) 135–224. [https://doi.org/10.1016/S0001-8686\(00\)00082-8](https://doi.org/10.1016/S0001-8686(00)00082-8).
- [16] L.J. Payer, IARC: An environmental approach to cancer research, *Science* (80-.). 178 (1972) 844–846. <https://doi.org/10.1126/science.178.4063.844>.
- [17] D. Ferber, J. Kaiser, Lashed by critics, WHO’s cancer agency begins a new regime, *Science* (80-.). 301 (2003) 36–37.

- <https://doi.org/10.1126/science.301.5629.36>.
- [18] The IARC Monographs Program: Changing Attitudes towards Public Health, *Int. J. Occup. Environ. Health.* 8 (2002) 144–152.
<https://doi.org/10.1179/107735202800338993>.
- [19] Z. Modrzejewska, W. Sujka, M. Dorabialska, R. Zarzycki, Adsorption of Cr(VI) on Cross-Linked Chitosan Beads, *Sep. Sci. Technol.* 41 (2006) 111–122.
<https://doi.org/10.1080/01496390500446160>.
- [20] V.M. Boddu, K. Abburi, J.L. Talbott, E.D. Smith, Removal of hexavalent chromium from wastewater using a new composite chitosan biosorbent, *Environ. Sci. Technol.* 37 (2003) 4449–4456.
<https://doi.org/10.1021/es021013a>.
- [21] S. Babel, T.A. Kurniawan, Low-cost adsorbents for heavy metals uptake from contaminated water: A review, *J. Hazard. Mater.* 97 (2003) 219–243.
[https://doi.org/10.1016/S0304-3894\(02\)00263-7](https://doi.org/10.1016/S0304-3894(02)00263-7).
- [22] G. Asgari, A.R. Rahmani, J. Faradmali, A. Motaleb, S. Mohammadi, Kinetic and Isotherm of Hexavalent Chromium Adsorption onto Nano Hydroxyapatite, 2012. www.umsha.ac.ir/jrhs (accessed June 15, 2020).
- [23] Y. Nishiyama, T. Hanafusa, J. Yamashita, Y. Yamamoto, T. Ono, Adsorption and removal of strontium in aqueous solution by synthetic hydroxyapatite, *J. Radioanal. Nucl. Chem.* 307 (2016) 1279–1285.
<https://doi.org/10.1007/s10967-015-4228-9>.
- [24] S.S. Metwally, I.M. Ahmed, H.E. Rizk, Modification of hydroxyapatite for removal of cesium and strontium ions from aqueous solution, *J. Alloys Compd.* 709 (2017) 438–444.
<https://doi.org/10.1016/j.jallcom.2017.03.156>.
- [25] S. Zamani, E. Salahi, I. Mobasherpour, Removal of Nickel from Aqueous Solution by Nano Hydroxyapatite Originated from Persian Gulf Corals, 1 (2013) 173–190.
<https://doi.org/10.13179/canchemtrans.2013.01.03.0033>.
- [26](a) E. Opoku, Progress on Homogeneous Ruthenium Complexes for Water Oxidation Catalysis: Experimental and Computational Insights, *J. Chem. Rev.* 2 (2020) 211–227.
<https://doi.org/10.33945/SAMI/JCR.2020.4.1>. (b) B. Donkor, E. Opoku, (2020). Formation of Steroid-Type Skeletons: An Ubiquitous Natural Product. *Advanced J. Chem-Sec. B*, 2(4), 209–213. doi: 10.33945/SAMI/AJCB.2020.4.5.
- [27] A. Chandrasekar, S. Sagadevan, A. Dakshnamoorthy, Synthesis and characterization of nano-hydroxyapatite (n-HAP) using the wet chemical technique, *Int. J. Phys. Sci. Full Length Res. Pap.* 8 (2013) 1639–1645.
<https://doi.org/10.5897/IJPS2013.3990>.
- [28] H. Gheisari, E. Karamian, M. Abdollahi, A novel hydroxyapatite -Hardystonite nanocomposite ceramic, *Ceram. Int.* 41 (2015) 5967–5975.
<https://doi.org/10.1016/j.ceramint.2015.01.033>.
- [29] E. Nejati, H. Mirzadeh, M. Zandi, Synthesis and characterization of nano-hydroxyapatite rods/poly(l-lactide acid) composite scaffolds for bone tissue engineering, *Compos. Part A Appl. Sci. Manuf.* 39 (2008) 1589–1596.
<https://doi.org/10.1016/j.compositesa.2008.05.018>.
- [30] S. Shahabi, F. Najafi, A. Majdabadi, T. Hooshmand, M.H. Nazarpak, B. Karimi, S.M. Fatemi, Effect of Gamma Irradiation on Structural and Biological Properties of a PLGA-PEG-Hydroxyapatite Composite, (2014).

- <https://doi.org/10.1155/2014/420616>.
- [31] A. Günay, E. Arslankaya, I. Tosun, Lead removal from aqueous solution by natural and pretreated clinoptilolite: Adsorption equilibrium and kinetics, *J. Hazard. Mater.* 146 (2007) 362–371. <https://doi.org/10.1016/j.jhazmat.2006.12.034>.
- [32] I. Langmuir, The constitution and fundamental properties of solids and liquids. II. Liquids, *J. Am. Chem. Soc.* 39 (1917) 1848–1906. <https://doi.org/10.1021/ja02254a006>.
- [33] N. Ayawei, A. Ekubo, D.W.-O.J. of, undefined 2015, Adsorption of congo red by Ni/Al-CO₃: Equilibrium, thermodynamic and kinetic studies, *Orientjchem.Org.* (n.d.). <http://www.orientjchem.org/vol31no3/adsorption-of-congo-red-by-nial-co3-equilibrium-thermodynamic-and-kinetic-studies/> (accessed June 13, 2020).
- [34] M.R. Matsumoto, Modeling cadmium adsorption by activated carbon using the langmuir and freundlich isotherm expressions, *Sep. Sci. Technol.* 28 (1993) 2179–2195. <https://doi.org/10.1080/01496399308016742>.

HOW TO CITE THIS ARTICLE

Aborode Abdullahi Tunde, Benedicta Donkor, Abigail Owusuwaa Gyamfi and Ernest Opoku, Isotherms, Kinetics, Equilibrium, and Thermodynamics Studies on the Uptake of Hexavalent Chromium Ions from Aqueous Solution Using Synthetic Hydroxyapatite, *Ad. J. Chem. B*, 2 (2020) 214-225

DOI: [10.22034/ajcb.2020.113974](https://doi.org/10.22034/ajcb.2020.113974)

URL: http://www.ajchem-b.com/article_113974.html

